THE USE OF SILICONE MATERIALS TO MODEL ABDOMIAL AORTIC ANEURYSM BEHAVIOUR

Barry J. Doyle,[1] Anthony Callanan,[1] Timothy J. Corbett,[1] Aidan J. Cloonan,[1] Michael R. O'Donnell,[1] David A. Vorp[2] and Timothy M. McGloughlin[1]

1. *Centre for Applied Biomedical Engineering Research (CABER), Department of Mechanical and Aeronautical Engineering, and Materials and Surface Science Institute, University of Limerick, Ireland.*

2. *Centre for Vascular Remodelling and Regeneration, McGowan Institute for Regenerative Medicine, University of Pittsburgh, USA.*

ABSTRACT

This paper aims to identify the rupture locations of abdominal aortic aneurysms. Dow Corning Sylgard 184 was mechanically characterised. Five idealised models were then manufactured using this silicone rubber which were subsequently inflated to rupture with the images recorded using a high speed camera. Four of the five models tested ruptured at inflection points in the proximal and distal regions of the aneurysm sac, and not at regions of maximum diameter.

INTRODUCTION

Aneurysms form a significant portion of cardiovascular related deaths in the Western world. Aneurysms are permanent and irreversible localised dilations [1], and although can form in any blood vessel, artery or vein, the more serious aneurysms occur in the abdominal aorta, the brain arteries, and the thoracic aorta. Approximately 500,000 AAAs are diagnosed worldwide each year [2] resulting in 15,000 deaths per year in the USA alone [3]. Typically, an AAA is surgically repaired once shown to have reached or exceeded a diameter of 5cm. There have been reports that this threshold may lead to inaccurate surgical-decision making as not only can smaller AAAs rupture [4-6], but also, large AAAs can remain stable [6]. It is known that by applying the definition of material failure to AAAs, the AAA will rupture when the locally acting wall stress exceeds the locally acting wall strength. Currently, much research is aimed at examining the wall stress distribution within the AAA wall [7-14]. Researchers have also examined methods to determine the strength of the AAA wall, both invasively from excised tissue [15-17] and non-invasively [18]. While there is much focus on attempting to numerically understand the mechanics of AAA rupture, only limited work has focussed on the development of experimental methods of determining rupture potential. The purpose of this study is to mechanically characterise a type of silicone rubber material to be used as the wall analogue of ideal AAA models, and to perform *in vitro* rupture studies to determine the site of rupture. Numerical modelling will attempt to quantify these experimental results.

METHODS

Material Characterisation

Dow Corning Sylgard 184 silicone rubber was used as the material for this study. Aluminium moulds were designed and manufactured to be used with the injection-method to create the silicone rubber samples. The mould cavity conforms to a Type 2 tensile test specimen as outlined in BS ISO 37. The test apparatus used was the Tinius Olsen (Surrey RH1 5DZ, England). For the tensile testing, a strain rate of 500mm/min was applied, as recommended in BS ISO 37 for Type 2 specimens. Preconditioning of each sample was also performed. An initial stretch-relax program of ten cycles to a 20% strain rate was carried out on each sample.

Rupture Modelling

In order to study the rupture of an aneurysm *in vitro*, the idealised AAA model developed and used extensively in previous research by our group [19-23] was utilised. Five AAA models to be used in the rupture study were manufactured using this technique.

The experimental rig consisted of a

mirrored-wall arrangement, pneumatic airline, pressure regulator, pressure manometer and high speed camera. The model was clamped to a retort stand and connected to the air supply with silicone tubing. A high speed camera (Olympus i-Speed, Olympus Corporation) was used to capture the point and location of rupture. The camera is capable of recording images at rates up to 33,000 frames per second (fps). A pixel resolution of 800 x 600 at 1000fps was deemed adequate for this application, and images were recorded using a monochrome lens. Once the AAA model was attached to the test rig, the high speed camera was adjusted to ensure optimum focus and angle. To determine the accuracy of the experimental tests, the evaluated material was implemented in the FEA software ABAQUS v6.7 (SIMULIA, R.I., USA) as the wall of the ideal AAA. Boundary conditions similar to the experimental set-up were implemented to the virtual AAA model.

RESULTS

Material Characterisation

Tensile testing revealed that the average UTS of Sylgard 184 is 7.7361 ± 1.6597 MPa, compared with 8.1 MPa on the specification sheet. In order to mechanically characterise the material, the experimental data from the tensile tests were converted to true stress and true strain, and then a 5th order polynomial curve was fitted to the data to obtain a mean experimental data curve, as shown in Figure 1.

The basic Ogden stain energy function [24] can be seen in Eqn.1, with the resulting material coefficients shown in Table 1.

$$W(\lambda_1,\lambda_2,\lambda_3)=\sum_{p=1}^{N}\frac{\mu_p}{\alpha_p}\left(\lambda_1^{\alpha_p}+\lambda_2^{\alpha_p}+\lambda_3^{\alpha_p}-3\right) \quad (1)$$

Table 1: Material coefficients for the third order Ogden model for Sylgard 184. D=0 for all constants.

	Mu	*Alpha*
1	-304.235	1.2667
2	148.232	1.5962
3	157.156	0.9075

The results of the FEA and the uniaxial tensile tests compared favourably, as shown in Figure 2. Therefore, confidence was established in the material characterisation of Sylgard 184.

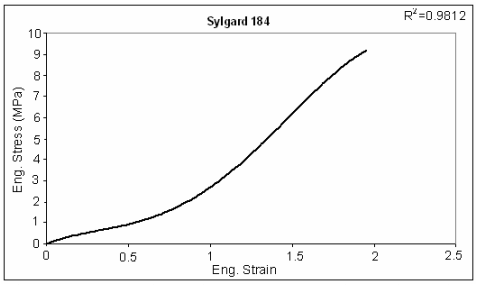

Figure 1: Engineering stress and engineering strain experimental data fit of 5th order polynomial curve for Sylgard 184.

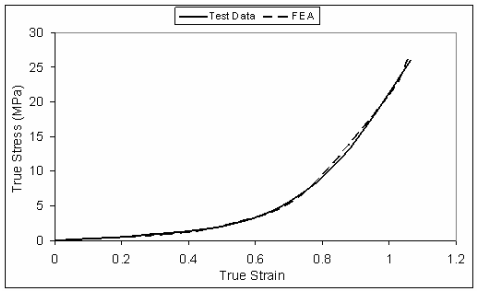

Figure 2: Comparison of results for the tensile tests and the numerical simulation of Sylgard 184.

Rupture Modelling

Of the five silicone models ruptured *in vitro*, four models experienced rupture at a region of inflection on the surface of the model. An inflection point is defined as points on the AAA surface at which the local AAA wall shape changes from concave outward to concave inward [25]. This finding is consistent with previous reports by our group [13,19,21] and others [25] that noted peak stresses at these regions instead of at the maximum diameter of the AAA. A summary of the rupture results can be seen in Table 2. Burst pressures were also recorded. One silicone model ruptured at the iliac bifurcation.

Table 2: Summary of experimental rupture results

Test	*Rupture Location*	*Rupture Pressure (mmHg)*
1	Proximal Inflection Point	254.7
2	Proximal Inflection Point	278.6
3	Proximal Inflection Point	466.2
4	Distal Inflection Point	278.7
5	Iliac Bifurcation	544.6

The sequence of events leading to rupture for *Test 1* can be seen in Figure 3. This illustration shows the frame where material failure initiates, leading to rupture of the model, and ultimately complete failure of the silicone model. It should be noted that no models failed along the 'seam' line of the silicone model from the manufacturing process. In Figure 3, *(A)* shows the inflated model, *(B)* the initial point of rupture, *(C)* propagation of the failure zone, and *(D)* complete failure of the silicone model. A similar sequence was observed for all four models that ruptured at regions of inflection.

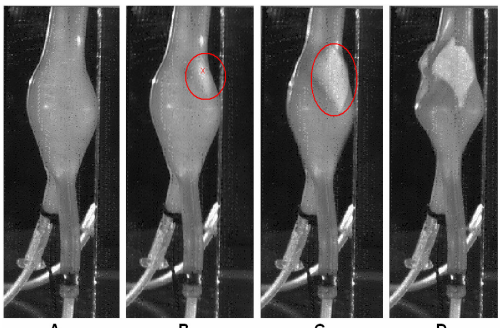

Figure 3: Sequence of events leading to model rupture of *Test 1*. The rupture location is highlighted in (B) and (C). A similar sequence was observed for all four models that ruptured at regions of inflection.

By implementing the material constants derived earlier, it was possible to simulate the experimental rupture study numerically. Stress distributions on the surfaces of the virtual AAA model reveal that high stresses occur at the regions of inflection and not at regions of maximum diameter. This has been proven by our group both numerically using the finite element method [21] and experimentally using the photoelastic method [19].

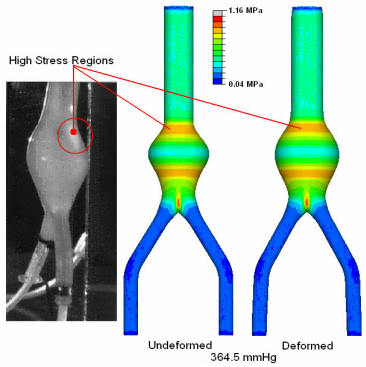

Figure 4: *In vitro* rupture locations and FEA stress patterns. High stress occurs at inflection points which correlate with rupture locations in experimental models.

DISCUSSION

The focus of this paper was to experimentally rupture rubber ideal AAA models in order to observe burst locations. There has been little reported on the *in vitro* rupture of abdominal aortic aneurysms, with much focus on the computational analysis of these aneurysms [7-14]. Morris et al. [19] observed rupture locations at the inflection regions during the use of the photoelastic method. Five models were manufactured using a technique developed by our group [22,23]. The commercially available silicone rubber Sylgard 184 from Dow Corning was used as an analogue for the AAA wall. Silicone rubber is an appropriate analogue for arterial tissue and has been used in previous studies [22,23,26,27]. Tensile testing revealed that the UTS of the material (mean ± standard deviation) is 7.7361 ± 1.6597 MPa. By fitting a polynomial curve to the experimental data and evaluating the material using ABAQUS v6.7, material coefficients were determined. The optimum strain-energy function for this particular material is a third-order Ogden function as shown in Eqn. 1, and allows the material to remain stable at all stresses and strains.

The use of a high-speed camera to record the point of rupture proved to be a very powerful experimental tool. The optimum image resolution was found to be 1000fps. Air pressure was increased incrementally until the point of rupture. Rupture pressures varied significantly for two of the five models, as shown in Table 2. Mean rupture pressure was 364.56 ± 131.89 mmHg. Three models experienced rupture at the proximal inflection region, one at the distal inflection point, and one model ruptured at the iliac bifurcation. Rupture studies were then replicated using the finite element method. Similar boundary conditions were used to those *in vitro*. Comparing the experimental rupture locations with the high stress regions found using FEA showed good correlation, as shown in Figure 6.

CONCLUSION

Ideal AAA models ruptured at regions of inflection and not at areas of maximum diameter. This is consistent with predicted results. The use of a high speed camera is a useful experimental tool in monitoring rubber AAA rupture locations. To improve the

method described, more suitable arterial analogues that mimic arterial properties more closely are required, thus possibly leading to an improved understanding of AAA rupture.

ACKNOWLEDGEMENTS

The authors would like to thank (i) the Irish Research Council for Science, Engineering and Technology (IRCSET) Grant RS/2005/340 (ii) Grant #R01-HL-060670 from the US National Heart Lung and Blood Institute (iii) Dr. Liam Morris from the Galway Medical Technology Centre, GMIT, Ireland (iv) Kevin O'Flanagan from the Department of Manufacturing and Operation Engineering, University of Limerick, Ireland, for his assistance with the high-speed imaging (v) Maria Ryan for her help with the experimental rupture modelling (vi) the Department of Vascular Surgery in the Midwestern Regional Hospital, Ireland, in particular, Mr. Eamon Kavanagh, Mr. Paul Burke and Prof. Pierce Grace (vii) Samarth Shah from the Centre for Vascular Remodelling and Regeneration, University of Pittsburgh, USA and (viii) Michel S. Makaroun, MD, Department of Surgery, University of Pittsburgh, USA.

REFERENCES

1. N Sakalihasan, R Limet and OD Defawe. *Lancet*. **365**(9470):1577-89 (2005).
2. JP Vande Geest, MS Sacks, DA Vorp. *Journal of Biomechanics*. **39**:2347-2354 (2006).
3. C Kleinstreuer, Z Li. Biomedical Engineering Online. **5**:19 (2005).
4. SC Nicholls, JB Gardner, MH Meissner et al. *Journal of Vascular Surgery*. **28**:884-888 (1998).
19. Biomedical Engineering. **34**:7:1098-1106 (2006).
20. L Morris, P O'Donnell, P Delassus, et al. Strain. **40**:165-172 (2005).
21. EUROSTAR Data Registry Centre, 2001. R Laheij, C van Marrewijk, J Buth.
22. A Callanan, LG Morris, TM McGloughlin. *European Society of Biomechanics*. S-Hertogenbosch, Netherlands (2004).
23. HS Flora, B Talie-Faz, L Ansdell, et al. *Journal of Endovascular Therapy*. **9**:665-675 (2002).
5. RC Darling, CR Messina, DC Brewster, et al. *Circulation.* **56**(II):161-164 (1997).
6. DA Vorp. *Journal of Biomechanics*. **40**:1887-1902 (2007).
7. ML Raghavan, DA Vorp, MP Federle, et al. *Journal of Vascular Surgery*. **31**:760-769 (2000).
8. AK Venkatasubramaniam, MJ Fagan, T Mehta, et al. *European Journal of Vascular and Endovascular Surgery*. **28**:168-176 (2004).
9. MF Fillinger, SP Marra, ML Raghavan, et al. *Journal of Vascular Surgery*. **37**:724-732 (2003).
10. MF Fillinger, ML Raghavan, SP Marra, et al. *Journal of Vascular Surgery*. **36**:589-597 (2002).
11. M Truijers, JA Pol, LJ SchultzeKool, et al. *European Journal of Vascular and Endovascular Surgery*. **33**:401-407 (2007).
12. WR Mower, WJ Quinones, SS Gambhir. *Journal of Vascular Surgery*. **26**:602-608 (1997).
13. BJ Doyle, A Callanan, TM McGloughlin. Biomedical Engineering Online. **6**:38 (2007).
14. JF Rodriguez, C Ruiz, M Doblare, et al. Journal of Biomechanical Engineering. **130**:021023-1-10 (2008)
15. MJ Thubrikar, M Labrosse, F Robicsek, et al. *Journal of Medical Engineering and Technology*. **25**(4):133-142 (2001).
16. ML Raghavan, MW Webster, DA Vorp. Annals of Biomedical Engineering . **24**:573-582 (1996).
17. ML Raghavan, J Kratzberg, EMC de Tolosa, et al. Journal of Biomechanics. **39**(16):3010-6 (2006).
18. JP Vande Geest, DHJ Wang, SR Wisniewski, et al. Annals of
24. BJ Doyle, LG Morris, A Callanan, et al. *Journal of Biomechanical Engineering*. **130**:034501-5 (2008).
25. T O'Brien, L Morris, P O'Donnell, et al. *Pro. IMechE. (H) Journal of Engineering in Medicine*. **219**. (2005)
26. RW Ogden. *Non-linear elastic deformations*. Mineola, New York: Dover Publication Inc. (1984).
27. DA Vorp, ML Raghavan, MW Webster. *Journal of Vascular Surgery*. **27**(4):632-639 (1998).
28. PALS Marins, RM Natal Jorge, AJM Ferreira. *Strain*. **42**:135-147 (2006).

29. OA Shergold, NA Fleck, D Radford. *International Journal of Impact Engineering*. **32**:1384-1402 (2006).
30. DHJ Wang, MS Makaroun, MW Webster, et al. *Journal of Vascular Surgery*. **36**:598-604 (2002).
31. GW Schurink, JM van Baalen, MJ Visser, et al. *Journal of Vascular Surgery*. **31**:501-506 (2000).